Nature of the liquid crystalline phase transitions in the cesium pentadecafluorooctanoate (CsPFO)–water system: The nematic-to-isotropic transition

K. W. Jolley and M. H. Smith
Institute of Fundamental Sciences, Massey University, Palmerston North, New Zealand

N. Boden
Centre for Self-Organising Molecular Systems and School of Chemistry, University of Leeds, Leeds LS2 9JT, United Kingdom

J. R. Henderson
Centre for Self-Organising Molecular Systems and Department of Physics and Astronomy, University of Leeds, LS2 9JT, United Kingdom

(Received 11 July 2000; published 20 April 2001)

Deuterium NMR spectroscopy of ^2H_2O has been used to monitor the magnetic-field-induced order on approaching a transition to a nematic phase in isotropic solutions of disklike micelles of cesium pentadecafluorooctanoate. Highly accurate data on the phase boundaries and spinodals have been obtained for solutions with volume fraction concentration ϕ between 0.078 and 0.201. The quantity $T_{IN}-T^*$, where T^* is the spinodal limit of the isotropic phase and T_{IN} is the temperature at which the nematic phase first appears on cooling, decreases linearly with decreasing concentration, extrapolating to zero only at zero concentration. Thus, there is no evidence to support the presence of a Landau point along the transition line as has previously been conjectured. The values for $(T_{IN}-T^*)/T_{IN}$ are in the range $10^{-5}-10^{-4}$, up to two orders of magnitude smaller than corresponding values reported for calamitic thermotropic nematics. The transition gap $(\phi_{NI}-\phi_{IN})/\phi_{IN}\sim 0.33\%$ for $\phi<0.20$ is also very small, although finite as required for a first-order phase transition. These data, when combined with previously measured properties, present an intriguing picture of the isotropic-to-nematic phase transition in a paradigmatic system of self-assembled diskotic particles. However, it is not completely clear, within the context of current theoretical understanding, whether the behavior of this system is explicable by hard-particle models, or if the self-assembly plays a crucial role in weakening the phase transition.

DOI: 10.1103/PhysRevE.63.051705 PACS number(s): 64.70.Md

I. INTRODUCTION

Salts of short-chain perfluorocarboxylic acids form aqueous solutions of disklike micelles which are exceptionally stable over wide concentration intervals. With increasing concentration the disklike micelles undergo a sequence of ordering transitions to, first, a nematic N_D phase and, subsequently, a smectic lamellar phase [1–8]. These transitions have been attributed to predominantly hard-particle interactions between the micelles [6]; that is, the isotropic-to-nematic transition occurs when the surfactant volume fraction concentration ϕ attains a critical proportion of the axial ratio $e=a/b$ of the micelles, where a is the length of the minor or symmetry axis (2.2 nm [9]), and b the length of the major or perpendicular axis. The form of the temperature-versus-composition phase diagram is therefore determined by the factors that govern the variations of the size of the micelle with temperature and composition. The archetypal surfactant is cesium pentadecafluorooctanoate (CsPFO). A partial phase diagram for the CsPFO–D_2O system was published in 1979 [1], and a more detailed and complete version, reproduced in Fig. 1, in 1987 [3]. The phase diagram in H_2O is very similar but with the transition temperatures a few degrees lower [5]. Changing the counterion from Cs^+ to NH_4^+ or $N(CH_3)_4^+$ simply shifts the liquid crystal phase transition temperatures, at comparable volume fractions, to lower temperatures [7], although in the case of the Li^+ salts the aggregate structures and behavior are more complex [10].

In the CsPFO–D_2O system the N_D^+ phase is stable for weight fractions w between 0.225 ($\phi=0.121$) and 0.632 ($\phi=0.449$) and temperatures T between 285.3 and 351.2 K. It is characterized by long-range correlations in the orientations of the symmetry axes of the micelles. The N_D^+-to-L_D transition is characterized by an apparent tricritical point T_{cp} ($w=0.43$; $\phi=0.263$; $T=304.8$ K). The transition is perceived to involve solely the positional ordering of the micelles onto planes arranged periodically along the nematic director **n**, and, as such, L_D is referred to as a diskotic lamellar phase. However, at higher concentrations of surfactant, as a consequence of micelle packing constraints and interlayer repulsive forces, a transition in aggregate structure is anticipated [11]. Here we focus on the mechanism of the I-to-N_D^+ transition.

Interest in phase transitions in the CsPFO–water systems stems from the opportunity to compare the behavior with that for thermotropic liquid crystals, on the one hand, and that predicted by hard-particle models on the other. Micellar systems are unique in that the internal structure of a micelle is not necessarily conserved at a transition, and this may lead to coupling between internal (micellar) and external (order parameter) degrees of freedom. These issues have stimulated many studies of the I-to-N_D^+ transition [12–25]. The width of the biphasic region is seen to be experimentally narrow (Fig. 1) suggesting that the transition may be very weak. This has

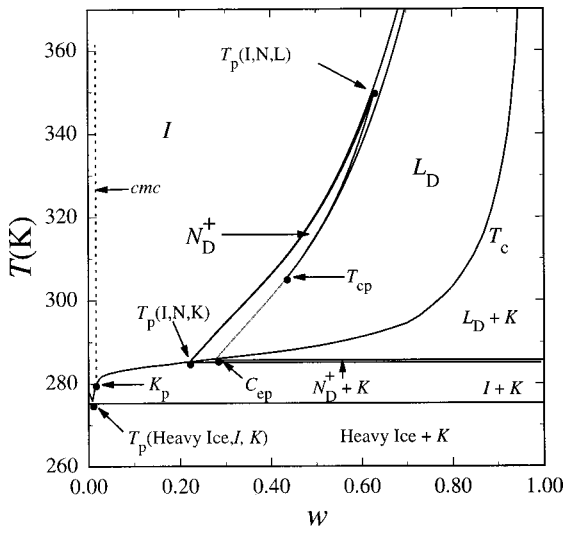

FIG. 1. Phase diagram for the CsPFO–D_2O system. Nomenclature: *I*, isotropic micellar solution phase [to the right of the critical micelle concentration (cmc) line]; N_D^+, discotic nematic phase with positive diamagnetic susceptibility; L_D, discotic lamellar phase; *K*, CsPFO crystal; T_{cp}, the lamellar-nematic tricritical point; T_p (heavy ice, *I,K*), the heavy-ice–isotropic-solution–crystal triple point; $T_p(I,N,K)$, the isotropic-micellar–nematic–crystal triple point; $T_p(I,N,L)$, the isotropic-micellar-solution–nematic–lamellar triple point; C_{ep}, the critical end point; K_p, the Krafft point; T_c, the solubility curve.

led to measurements of $T_{IN}-T^*$ [15,17,26], where T^* is the extrapolated supercooling limit of the isotropic phase and T_{IN} is the temperature at which the nematic phase first appears on cooling. This quantity has been found to decrease as w decreases and to be below 25 mK at $w=0.30$ [17], the lowest concentration of the measurements. This was an unexpected result because $T_{IN}-T^*$ is typically of the order of 1 K for thermotropic nematics [27] and similarly for the N_D^- (negative diamagnetic susceptibility) phase of the decylammonium chloride/ammonium chloride/water system [28]. The observed concentration dependence of $T_{IN}-T^*$ led to arguments that the transition may be approaching second-order behavior at a Landau point associated with a crossover from uniaxial to biaxial behavior, a conclusion seemingly supported by latent heat measurements [24]. However, there is no indication in the phase behavior (Fig. 1) for the existence of such a point.

Earlier studies of $T_{IN}-T^*$ were based on measurements of the Cotton-Mouton coefficient, which cease to be practicable below $w=0.3$. A more precise deuterium NMR method has been shown to be applicable to the CsPFO–D_2O system at this concentration and yielded a value of 0.016(2) K at $w=0.302$ [26]. We now report similar measurements to lower concentrations. In particular, we have been able to make measurements in supercooled samples below $w=0.221$ and to extend measurements down to $w=0.150$ ($\phi=0.078$) in this manner. These results show that $T_{IN}-T^*$ decreases linearly with decreasing concentration of CsPFO from 0.018(2) K at $w=0.345$ ($\phi=0.201$) to 0.010(2) K at $w=0.150$ ($\phi=0.078$), extrapolating to zero at infinite dilution. The quantity T^+-T_{NI}, where T_{NI} is the lower-temperature limit of the nematic/isotropic coexistence region and T^+ the superheating limit of the nematic phase, behaves similarly [25]. Thus, the transition is unequivocally first order over its entirety. It is not clear whether this behavior is explicable by hard-particle models or if the self-assembly plays a significant role in weakening the phase transition.

II. MATERIALS AND METHODS

A. Sample preparation

CsPFO was prepared by neutralizing aqueous solutions of pentadecafluorooctanoic acid (Aldrich Chemical Company Inc.) with cesium carbonate (BDH, Ltd.). The neutralized solution was freeze dried and the salt recrystallized twice from 50% v/v *n*-butanol/*n*-hexane. Residual solvent was removed by heating the salts to 30 °C under vacuum (5×10^{-4} bar) for longer than 48 h. Deuterium oxide (Aldrich 99.6 at. % D) was used without further purification.

NMR samples were prepared by weighing CsPFO and D_2O directly into 5 mm o.d. NMR tubes, to a precision of 0.000 02 g, using a Mettler AT 261 Delta Range balance. The sample tubes were then flame sealed to lengths of about 50 mm. All samples gave consistent NMR measurements over the period of the study providing care was taken to ensure homogeneous mixing of samples in the isotropic phase prior to measurement.

B. NMR measurements

^{2}H NMR spectra were measured with a JEOL GX270 spectrometer operating at 41.34 MHz. ^{2}H spectra were obtained using 16 000 data points over a frequency range of 1.0 kHz at a frequency resolution of 0.125 Hz per data point. Four accumulations at a repetition rate of 2 s were used for all spectra. Sample temperatures were regulated using a computer controlled double-pass water-flow sample thermostat [29]. This minimized temperature gradients and enabled the temperature to be controlled to a precision of ±0.005 K. For samples having isotropic-to-nematic transition temperatures above the solubility curve, i.e., above $w=0.221$, typically periods of 10–12 min were allowed for the sample to reach thermal equilibrium, following each temperature decrement, before measurement of spectra. The temperature remained stable to within 0.001 K during measurements. However, for samples having w between 0.150 and 0.221, the isotropic-to-nematic transition temperatures lie below the solubility curve and they have a tendency to crystallize, a tendency that increases with dilution. The waiting time was, therefore, reduced to about 5 min at which time the temperature had been stable for at least 1 min. In the case of the $w=0.200$ sample, this procedure enabled all data to be collected in a single sweep before crystallization occurred. But for the $w=0.150$ sample crystallization occurred after about 15 min and it was necessary to reheat and remix the sample several times in order to collect all the data.

III. EXPERIMENTAL RESULTS

Measurements have been made along the isopleths depicted in Fig. 2, at concentrations w of 0.150, 0.200, 0.251,

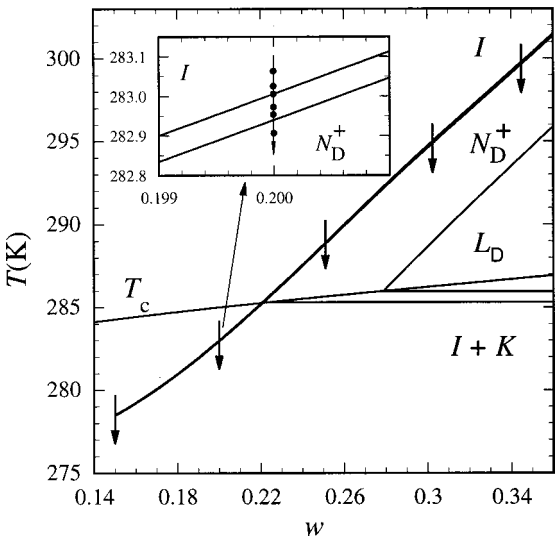

FIG. 2. Partial phase diagram for CsPFO–D_2O system showing the location of the I-to-N_D transition over the concentration range accessed in this study. The points on the isopleth at $w=0.200$ (expanded in the inset) represent the temperatures of the spectra shown in Fig. 3. The nematic phases for both the $w=0.200$ and 0.150 samples were accessed by supercooling below the solubility curve T_c.

0.302, and 0.345. The sequence of spectra observed in each case are very similar and typified by those for the $w=0.200$ sample in Fig. 3. At a temperature about 150 mK above T_{IN} the spectrum is a single line with a full width at half maximum, determined by spin lattice relaxation processes, of about 1.2 Hz. As the temperature is lowered toward T_{IN} the line begins to broaden (a) before splitting into a doublet whose separation increases rapidly in magnitude (b), (c) until T_{IN} is reached, at which point the splitting is quenched (d), (e). Below T_{IN} an outer doublet signifies the presence of the nematic phase (d). On continuing to cool the proportion of nematic to isotropic phase signal increases until at temperatures below T_{NI} only the nematic phase signal is present (f).

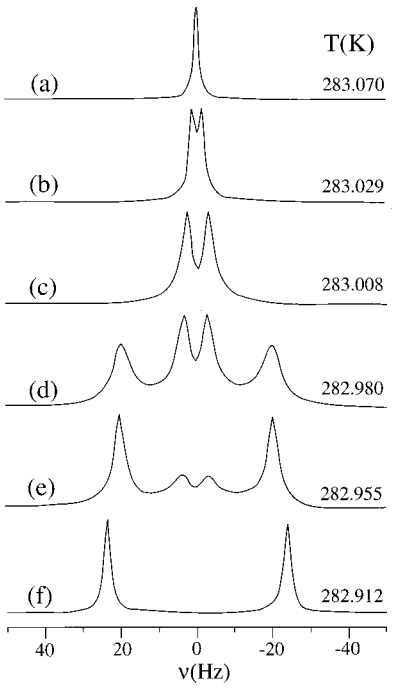

FIG. 3. Sequence of spectra observed on cooling a sample with $w=0.200$ from the I phase into the I/N_D biphasic region, along the isopleth shown in the inset of Fig. 2.

The splitting of the ^2H (D_2O) signal in the isotropic phase into a doublet arises from the orientational ordering of the micelles induced by coupling with the applied magnetic field,

$$U_{mag}(\cos\theta)=\frac{-\Delta\chi B^2}{3}P_2(\cos\theta), \tag{1}$$

and enhanced by the build-up in angular correlations of the micelles,

$$U_{mic}(\cos\theta)=\epsilon\overline{P}_2P_2(\cos\theta), \tag{2}$$

as T_{IN} is approached from above. Here $\Delta\chi$ is the anisotropy in the magnetic susceptibility of a micelle, θ is the angle between the micellar symmetry axis and the applied magnetic field, and ϵ is the Maier-Saupe mean field anisotropic interaction parameter. $\overline{P}_2$ is the second-rank orientational order parameter $\overline{P_2(\cos\theta)}$ and it is related to the induced quadrupole splitting $\Delta\tilde{\nu}$ by

$$\Delta\tilde{\nu}=\tfrac{3}{2}|\tilde{q}_{zz}|_s\overline{P}_2, \tag{3}$$

where $|\tilde{q}_{zz}|_s$ is the partially averaged component of the deuterium nuclear-quadrupole electric-field-gradient interaction tensor measured parallel to B when $\overline{P}_2$ is 1. To relate $\overline{P}_2$ to ϵ, we have adopted the approach of Luckhurst [30,31] to give

$$\overline{P}_2=\left(\epsilon\overline{P}_2+\frac{\Delta\chi B^2}{3}\right)\Big/ /5k_BT$$

which, on rearrangement, becomes

$$\overline{P}_2=\Delta\chi B^2/15k_B(T-T^*) \tag{4}$$

where $T^*=\epsilon/5k_B$. Combining Eqs. (3) and (4) gives

$$\Delta\tilde{\nu}=\tfrac{3}{2}|\overline{q}_{zz}|_s\Delta\chi B^2/15k_B(T-T^*). \tag{5}$$

Over the narrow temperature interval (80 mK) for which quadrupole splittings are measured, the values of $|\tilde{q}_{zz}|_s$ and $\Delta\chi$ can be considered constant. Thus, the splittings are predicted to depend on B^2 and to diverge at T^* as illustrated in Fig. 4. The values of T_{IN} and of $T_{IN}-T^*$ obtained in this way are summarized in Table I.

The magnetic-field-induced quadrupole splitting has exactly the same origin as the field-induced optical birefringence. Yet none of the plots shown in Fig. 4 exhibits the nonlinearity observed in plots of optical birefringence against B^2 used to extract order parameter susceptibilities

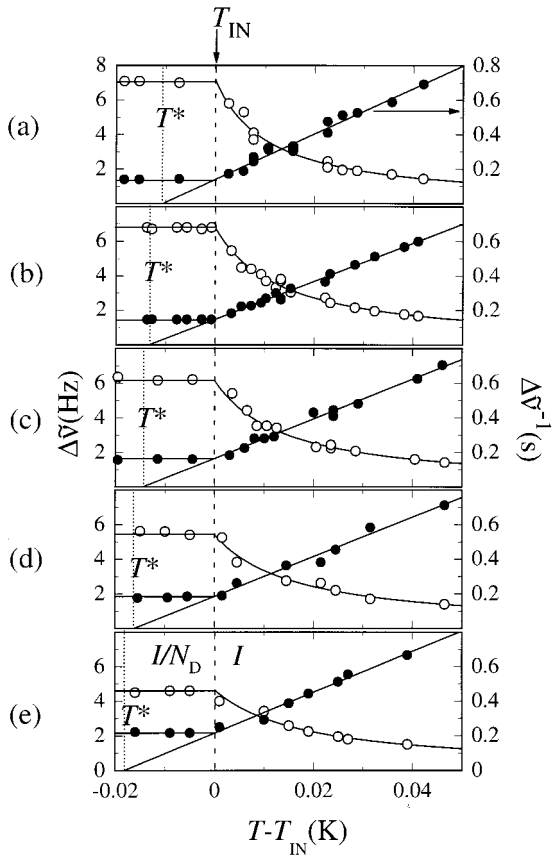

FIG. 4. Plots of $\Delta\tilde{\nu}$, the field-induced ^{2}H quadrupole splittings of ^2H_2O (open symbols), and its inverse $1/\Delta\tilde{\nu}$ (closed symbols) versus temperature in the I and the I/N_D biphasic regions for CsPFO–D_2O samples having weight fractions of (a) 0.150, (b) 0.200, (c) 0.251, (d) 0.302, and (e) 0.345. The discontinuity in the temperature dependence of both the $\Delta\tilde{\nu}$ and $\Delta\tilde{\nu}^{-1}$ plots characterizes T_{IN} and extrapolation of $\Delta\tilde{\nu}^{-1}$ to zero gives T^* (see Table I). The solid lines through the experimental measurements were obtained from least-squares fits of Eq. (5) to the $\Delta\tilde{\nu}^{-1}$ versus T data.

[15], indicative of the contribution of a second-order term to the measured birefringence. This second-order term is particularly important at high B and at temperatures close to T_{IN}. It would seem that at the magnetic flux density used in the present study (6.34 T) second-order terms are unimportant.

The lower concentration limit of measurement, $w=0.150$, is determined by the ability to supercool samples below T_c for a length of time commensurate with carrying out the measurements. For the $w=0.150$ sample, crystallization begins about 15 min after cooling below T_{IN}. For samples with lower concentrations, cooling to even lower temperatures is needed and the crystallization process occurs too quickly for measurements to be made. The upper concentration limit is determined by the temperature range over which field-induced ordering can be observed. The measured quadrupole splitting $\Delta\tilde{\nu}$ at T_{IN} decreases with increasing concentration (Table I) due to a lowering of the axial ratio e and a raising of $T_{IN}-T^*$. For the $w=0.345$ sample at 6.34 T $\Delta\tilde{\nu}$ is only 4.6 Hz. For samples with concentrations greater than this, the magnitude of the splitting is too small to obtain accurate measurements over a sufficiently wide temperature interval.

IV. DISCUSSION

In this paper we present a set of measurements over a concentration range that extends to far lower concentrations that those previously reported [15,17]. These measurements leave no room for the presence of a continuous phase transition at low concentrations; the transition gap as measured by $T_{IN}-T^*$, T^+-T_{NI}, or $\phi_{NI}-\phi_{IN}$ extrapolates to zero only at a hypothetical zero concentration point. This extrapolation also has interesting implications for statistical mechanical models which we therefore discuss in some detail below, together with the implications for simulation studies.

A. Micelle size along the I-to-N_D^+ transition line

In the ensuing interpretation of the experimental measurements values of the micelle size and shape are required. The direct information available at present for the CsPFO–D_2O system has come from x-ray measurements [32,33]. They show that, in the isotropic phase the micelles are disklike, and that, with increasing surfactant concentration at fixed temperatures, their size increases at first and then either remains constant or decreases slightly. There are more dramatic decreases in size as the temperature is raised at fixed concentrations. However, these results have been contradicted recently by claims that NMR self-diffusion measurements suggest that the micelle size actually increases with increasing temperature [34]. The NMR measurements of field-induced ordering are very sensitive to variations in micelle size and can be employed to resolve this paradox.

TABLE I. Best fit parameters obtained by fitting Eq. (5) to the data shown in Fig. 4. The errors in parentheses are estimated from the standard deviations of the $1/\Delta\tilde{\nu}$ vs T plots of Fig. 4.

w	ϕ	T_{IN} (K)	$T_{IN}-T^*$ (K)	$T_{IN}-T_{NI}$ (K)	$\Delta\tilde{\nu}$ (Hz) at T_{IN}	Slope/(s K^{-1})
0.150	0.078	278.508(1)	0.010(2)	0.050(5)	7.3(2)	13(1)
0.200	0.106	283.006	0.013	0.066	6.8	11.1(6)
0.251	0.137	288.673	0.014	0.082	6.2	11.6(5)
0.302	0.170	294.839	0.016	0.105	5.6	11.4(8)
0.345	0.201	300.381	0.018	0.134	4.6	11.8(9)

TABLE II. Axial ratios and transition entropies for the isotropic-to-nematic transition in the CsPFO–D_2O system.

w	ϕ	a/b[a] ± 0.01	w	ϕ	ΔS ($J\,mol^{-1}\,K^{-1}$)[b]
0.150	0.078	0.19	0.400	0.240	3.7
0.200	0.106	0.21	0.450	0.280	4.4
0.251	0.138	0.23	0.500	0.322	4.5
0.302	0.171	0.25	0.550	0.367	4.4
0.345	0.201	0.27			

[a]The a/b ratios have been calculated from the field-induced NMR splittings (Table I) by normalizing to the x-ray data for the $w=0.35$ sample [32,51], as described in the text.

[b]Entropy changes per mole of micelles, calculated from the transition enthalpies [24] and micellar aggregation numbers at the transition, as determined from x-ray measurements [32,51].

The value of $\Delta\tilde{\nu}$ at T_{IN} is given by Eq. (5) with $T=T_{IN}$. The expression for $|\tilde{q}_{zz}|_s$ in this equation may be written [3]

$$|\tilde{q}_{zz}|_s=\langle P_2(\cos\alpha)\rangle_s\chi_D(x_A/x_W)n_bS_{OD} \tag{6}$$

where χ_D is the ^2H quadrupole coupling constant, n_b is the number of water molecules bound per amphiphile, x_A and x_W are, respectively, the mole fractions of amphiphile and water, and S_{OD} is an order parameter that represents the averaging due to local reorientation of the bound water molecules. The quantity $\langle P_2(\cos\alpha)\rangle_s$ accounts for the diffusive motion of the water molecules over the surface of the micelle. The anisotropy in the magnetic susceptibility of the micelle $\Delta\chi_m$ in Eq. (5) can be written in terms of the anisotropy in the magnetic susceptibility $\Delta\chi_A$ for individual amphiphile molecules as

$$\Delta\chi_m=n\Delta\chi_AS_A\langle P_2(\cos\alpha)\rangle_s, \tag{7}$$

where n is the aggregation number of the micelle and S_A is an order parameter that represents the orientation fluctuations of the amphiphile molecules within the micelle. Previous work [3] has shown that over the temperature and concentration ranges of the nematic phase the product $\chi_Dn_bS_{OD}$ in Eq. (6) is essentially constant. Making the further reasonable assumption that the product $\Delta\chi_AS_A$ in Eq. (7) is also constant, then the magnitude of $\Delta\tilde{\nu}$ at T_{IN} scales with $n\langle P_2(\cos\alpha)\rangle_s^2(x_A/x_W)/(T_{IN}-T^*)$. From the experimental data it is thus possible to compare the relative values of $n\langle P_2(\cos\alpha)\rangle_s^2$ for any two samples. Since $\langle P_2(\cos\alpha)\rangle_s$ is a function of the axial ratio a/b of the micelle [3], as is the value of n, the variation in a/b with dilution can be determined. The values of a/b shown in Table II for samples with $w<0.35$ have been determined by normalizing the NMR data to the x-ray data for the $w=0.35$ sample. These observations confirm the behavior predicted by the x-ray measurements, contrary to the results calculated from water molecule self-diffusion coefficients [34].

The change in micelle sizes on dilution can also be obtained from a comparison of the slopes of the $\Delta\tilde{\nu}^{-1}$ vs T plots (Table I) which scale with the quantity $[n\langle P_2(\cos\alpha)\rangle_s^2(x_A/x_W)]^{-1}$. The changes in a/b on dilution calculated by this method agree to within experimental error with those calculated from the changes in the magnitude of $\Delta\tilde{\nu}$.

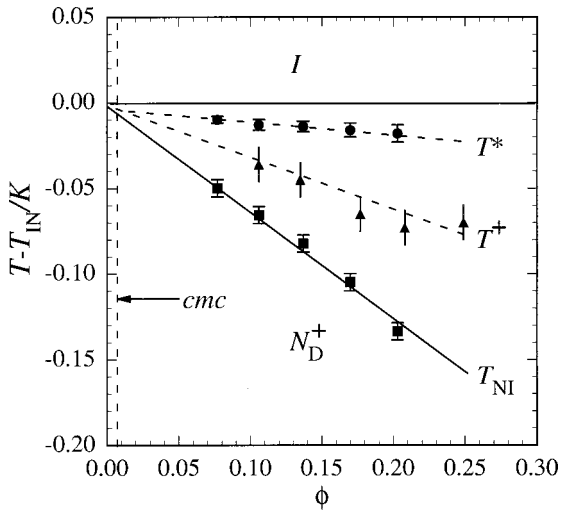

FIG. 5. Volume fraction dependence of T^*, T^+, and T_{NI} relative to T_{IN}. Values for $T_{IN}-T^*$ and $T_{IN}-T_{NI}$ are taken from Table I and those for T^+-T_{NI} from Ref. [25].

B. Nature of the nematic-to-isotropic transition

The concentration dependence of $T_{IN}-T^*$ as determined in the present study is displayed in Fig. 5. The data seem to indicate that $T_{IN}-T^*$ varies linearly with ϕ and extrapolates to zero as ϕ approaches zero. This is consistent, within experimental error, with values of T^+-T_{NI} obtained from the temperature dependence of the order parameter $S-S^+=k(T^+-T)^\beta$, where S^+ is the order parameter at the superheating limit T^+ to the nematic phase [25]. $T_{IN}-T_{NI}$ is also seen to be linearly proportional to ϕ. Therefore, the transition gap $\Delta\phi(\equiv\phi_{NI}-\phi_{IN})$ extrapolates to zero as ϕ approaches zero; see also Fig. 6. The T^* and T^+ lines are essentially spinodal lines for the nematic-to-isotropic transition. But this does not mean the transition is approaching a critical point at zero concentration; as long as $\Delta\phi/\phi$ remains finite, the transition remains first order. The isotropic-to-nematic transition will, in practice, end either before or at the critical micelle concentration. The important point, however, is that the narrowing of the transition is not associated with convergence on a tricritical, or Landau, point on dilution.

The low value of $(T_{IN}-T^*)/T_{IN}\sim10^{-5}-10^{-4}$ is up to two orders of magnitude smaller than corresponding values of $\sim10^{-3}$ reported for calamitic thermotropic nematics [35–38]. Even these values for thermotropics have proved a long-standing puzzle to theorists: the mean field prediction is 0.08 [39]. Thermally excited fluctuations have been invoked to render temperature dependence to the coefficients in the Landau–de Gennes free energy expression. This has led to improvements over the mean field results, but predictions are still short of the observed values [40]. So how can the even smaller values for $(T_{IN}-T^*)/T_{IN}$ for the diskotic micellar

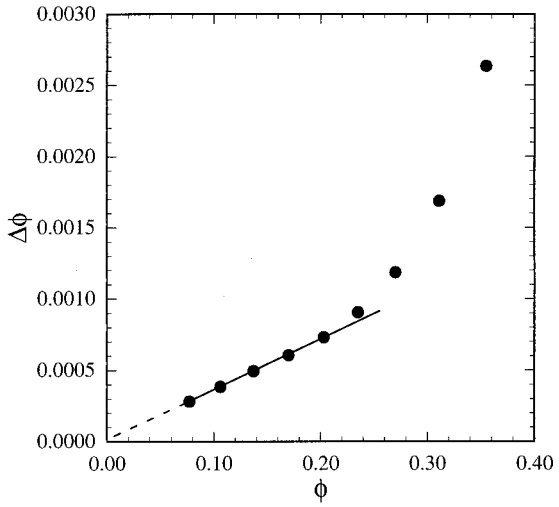

FIG. 6. Plot of $\Delta\phi$ ($\equiv\phi_{\mathrm{NI}}-\phi_{\mathrm{IN}}$) versus volume fraction of surfactant ϕ for the CsPFO–D_2O system.

system studied here be explained?

Micelles do not have a fixed size and shape. In aqueous solutions of the salts of perfluorinated surfactants the fluorosurfactant molecules continually exchange between the monomeric state and the micellar state at a rate of $\sim 10^{-6}\,\mathrm{s}^{-1}$ [41]. Thus, the intermicellar interactions are coupled to intramicellar degrees of freedom (self-assembly) and this could have a significant influence on fluctuations associated with the transition and consequently on the value of $(T_{\mathrm{IN}}-T^*)/T_{\mathrm{IN}}$. Indeed, we have previously reported a decrease of ~10% in a/b on going from isotropic to coexisting nematic phases [4,9]. This arises from the coupling between micellar self-assembly and the nematic order parameter. Polydispersity is also an important issue to bear in mind [42]. In the case of thermotropic liquid crystals, internal molecular conformational degrees of freedom could also be affecting fluctuations.

There are very few data available for the nematic-to-isotropic transition for thermotropic diskotics so that comparisons by necessity can only be made with thermotropic calamitics. For these, transition enthalpies are typically $0.5R$ and we see (Table II) that the values for the CsPFO–water system are very similar when the micelle is identified with the molecule, i.e., as the mesogenic particle. The NMR splittings (Fig. 4), which are proportional to the orientational order parameter, are seen to follow the mean field $(T-T^*)^{-1}$ law down to within at least 10 mK of T^*. Similar behavior is observed for thermotropic liquid crystals, at least down to within 1 K of T^*. For the nematic-to-isotropic transition $(T^+-T)^{\beta}$ law, calamitic thermotropic liquid crystals have been reported to show either the classical value of the order parameter exponent $\beta=0.5$ [43–45] or the tricritical value $\beta=0.25$ [46]. The value of β for CsPFO solutions is 0.34(2) along the entire N_D^+-to-I transition line, which has been linked to renormalization group theory [25]. This strong asymmetry of the transition is surprising for such a weak transition. Fluctuations [46] appear to be strongly influencing the transition on the nematic side but not on the isotropic side.

C. Comparison with hard-particle models

Monte Carlo simulations in a fluid of infinitely thin hard disks [47,48] have yielded a density jump of less than 2% across the isotropic-to-nematic transition [48]. This is potentially consistent with our observed value of $\Delta\phi/\phi=0.33\%$, for $\phi<0.20$, although recent work [42] appears to revise the simulation value upward to around 4%. The important point that follows from these simulation studies is that there is a definite asymmetry in the Onsager limit of disks versus rods. Only at the level of the second virial coefficient is there complete symmetry between ellipsoidal disks and rods. Here, the density jump is 27%, which is believed to be the true value for infinitely long rods. It follows that higher-order virial coefficients contribute to the qualitative nature of the hard-disk isotropic-to-nematic phase transition, such that the strength of the transition is greatly reduced. Accordingly, it is possible that hard-body models could explain our data. A crude method of attempting to incorporate the higher virial coefficients into an Onsager calculation is to use the y-expansion method [49]. For oblate ellipsoids at $a/b=0.364$, this has yielded a gap of 1.6%. Experiments on model colloidal systems [50], on the other hand, claim a significantly enhanced first-order nature (9%).

We can also compare the various predictions for the packing fraction at the transition and the values of the order parameter and its temperature exponent. Figure 7 compares the experimental packing fractions from our studies with those calculated from the y-expansion theory, for corresponding axial ratios. The micellar systems lie below the theoretical curve, perhaps appropriate to an even weaker transition. The dashed line shows an extrapolation to the infinitely thin disk limit, which is required if our data are to be fully explained by hard-body models. Whether or not this is indeed the case, or if the deviation at low concentration is due to additional physics such as attractive forces between the micelles, is unclear within current experimental error and theoretical understanding. The colloidal data of van der Kooij and Lekkerkerker [50] are at a significantly lower aspect ratio ($a/b=0.091$) and lies almost on the extrapolated y-expansion curve. The simulation value [47,48] for the nematic order parameter at the transition [$S=0.37(1)$] is consistent with our values only at high volume fraction [25]. The simulations also report tentative agreement with the tricritical value of the order parameter exponent on the nematic side ($\beta=0.25$), which differs from our previously published experimental value [$\beta=0.34(2)$] [25].

The above discussion shows that there remain a variety of intriguing questions concerning the nature of the isotropic-nematic phase transition for diskotics. Clearly, it would be helpful to revisit the hard-particle models to see if modern computing resources can rule out the very weak nature of the transition observed in our micellar systems. If so, there are plenty of reasons to explain such a discrepancy, including the presence of attractive interactions between the micelles, the coupling between self-assembly and the transition (the

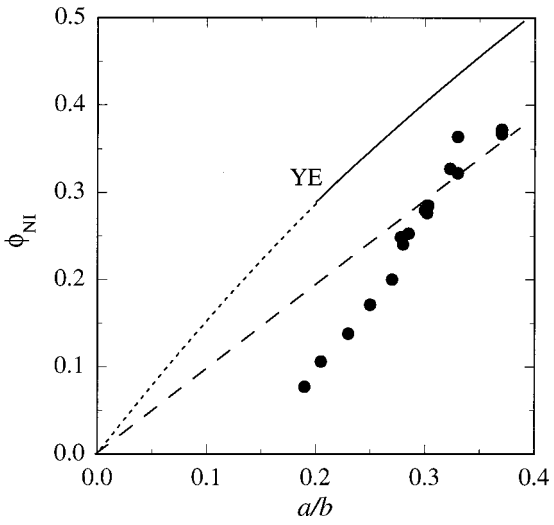

FIG. 7. Comparison of the nematic phase volume fractions and aggregate sizes at the isotropic-to-nematic transition with predictions of the Onsager model using the *y*-expansion (YE) technique (solid line; data supplied by B. Tjipto Margo). The dotted line is an extrapolation of these data using a quadratic fit. The dashed line through the experimental data and the origin indicates our suggested interpretation of the experimental data, in terms of hard-particle models. At volume fractions greater than 0.20 the a/b ratios are those obtained from average micellar volumes, obtained from x-ray measurements [32,51], assuming an a value of 2.2 nm [9]. The quality of the x-ray data was not sufficient to determine the aggregation distribution and hence quantify the amount of polydispersity. At lower volume fractions the a/b ratios were calculated from the field-induced-order splittings (Table II and text).

micelles are roughly 10% larger in the nematic phase than in the coexisting isotropic phase) including fluctuations, and the presence of polydispersity. With regard to the last point, it is worth noting that the simulations of Bates and Frenkel [42] failed to model the effect of the polydispersity that the colloidal systems are known to possess [50]. That is, simulation predicts an apparently unphysical dramatic widening of the transition region when polydispersity is incorporated, which would be even less applicable to our micellar data.

V. CONCLUSIONS

The isotropic-to-nematic transition in the CsPFO–water system has been established to be first order over the entire range of experimentally accessible concentrations $\phi \sim 0.07-0.40$. Moreover, $T_{IN}-T^*$, T^+-T_{NI}, and $(\phi_{NI}-\phi_{IN})$ are all found to vary linearly with ϕ (from $\phi<0.20$) and to extrapolate to zero only as ϕ approaches zero. Thus, there is no evidence to support the idea that a Landau point is being approached as previously conjectured [15,24]. Nevertheless, the transition appears to be extraordinarily weak: $(T_{IN}-T^*)/T_{IN}\sim 10^{-5}-10^{-4}$ compared to $\sim 10^{-3}$ in thermotropic systems. The entropy of the transition, however, when expressed as the entropy change per mole of micelles, is comparable to known values for thermotropic calamitic systems, $\Delta S\sim 0.5R$ (Table II), implying that the transition is not as weak as it may appear.

The extremely small gap $(\phi_{NI}-\phi_{IN})/\phi_{IN}\sim 0.33\%$ might possibly be explained by hard-particle models, but more theoretical or simulation work is needed here. The order parameter on the isotropic side follows the mean field $(T-T^*)^{-1}$ law to within 10 mK of the transition, similar to the behavior of thermotropic systems. But the order parameter exponent on the nematic side $\beta=0.34(2)$ differs from either the classical value 0.5 or the tricritical value 0.25, both of which have been claimed to apply to thermotropic systems. The tricritical value has also been obtained from Monte Carlo hard-disk simulations in the infinitely thin limit [47,48].

The explanation for the narrow spinodals and value of β could stem from fundamental differences in the fluctuations in micellar systems compared to typical thermotropic systems. The internal micellar structure represents an additional degree of freedom (self-assembly), which can couple to the order parameter and density fluctuations and lead to polydispersity. This could have a significant impact on the temperature dependence of the coefficients of the cubic and quartic order parameter terms in the Landau–de Gennes free energy expansion, in the vicinity of the transition. That is, one way to obtain an understanding of the impact of self-assembly on the transition would be to construct a free energy formulation using a Hamiltonian incorporating both intra- and intermicellar variables. Alternatively, maybe realistic simulation experiments will one day be practicable. In the meantime, it would clearly be worth returning to the simulation of infinitely thin hard disks, to see if modern computing resources can pin down the limiting value of $\Delta\phi/\phi$, in the absence of attractions, self-assembly, and polydispersity.

ACKNOWLEDGMENTS

The authors would like to thank B. Tjipto Margo for his *y*-expansion calculations plotted in Fig. 7, and one of us (J.R.H.) thanks M. P. Allen for helpful discussions.

[1] N. Boden, P. H. Jackson, K. McMullen, and M. C. Holmes, Chem. Phys. Lett. **65**, 476 (1979).
[2] N. Boden, K. Radley, and M. C. Holmes, Mol. Phys. **42**, 493 (1981).
[3] N. Boden, S. A. Corne, and K. W. Jolley, J. Phys. Chem. **91**, 4092 (1987).
[4] N. Boden, J. Clements, K. W. Jolley, D. Parker, and M. H. Smith, J. Chem. Phys. **93**, 9096 (1990).
[5] N. Boden, K. W. Jolley, and M. H. Smith, J. Phys. Chem. **97**, 7678 (1993).
[6] N. Boden *et al.*, J. Chem. Phys. **103**, 5712 (1995).
[7] J. P. Dombroski, P. J. B. Edwards, K. W. Jolley, and N. Boden, Liq. Cryst. **18**, 51 (1995).
[8] P. J. B. Edwards, K. W. Jolley, M. H. Smith, S. J. Thomsen, and N. Boden, Langmuir **13**, 2665 (1997).
[9] N. Boden *et al.*, J. Phys. (France) **47**, 2135 (1986).

[10] E. Everiss, G. J. T. Tiddy, and B. A. Wheeler, J. Chem. Soc., Faraday Trans. 1 **72**, 1747 (1976).
[11] R. Granek, W. M. Gelbart, Y. Bohbot, and A. Ben-Shaul, J. Chem. Phys. **101**, 4331 (1994).
[12] S. T. Chin and S. Kumar, Phys. Rev. Lett. **66**, 1062 (1991).
[13] M. R. Fisch, S. Kumar, and J. D. Litster, Phys. Rev. Lett. **57**, 2830 (1986).
[14] B. D. Larson and J. D. Litster, Mol. Cryst. Liq. Cryst. **113**, 13 (1984).
[15] C. Rosenblatt, S. Kumar, and J. D. Litster, Phys. Rev. A **29**, 1010 (1984).
[16] C. Rosenblatt, Phys. Rev. A **32**, 1115 (1985).
[17] C. Rosenblatt, Phys. Rev. A **32**, 1924 (1985).
[18] C. Rosenblatt and N. Zolty, J. Phys. (France) Lett. **46**, L1191 (1985).
[19] C. Rosenblatt, J. Phys. Chem. **91**, 3830 (1987).
[20] C. Rosenblatt, J. Phys. Chem. **92**, 5770 (1988).
[21] C. Rosenblatt, J. Colloid Interface Sci. **131**, 236 (1989).
[22] M. R. Kuzma, W. M. Gelbart, and Z.-Y. Chen, Phys. Rev. A **34**, 2531 (1986).
[23] G. Swislow, D. Schwartz, B. M. Ocko, P. S. Pershan, and J. D. Litster, Phys. Rev. A **43**, 6815 (1991).
[24] S. T. Shin, S. Kumar, D. Finotello, S. Sabol Keast, and M. E. Neubert, Phys. Rev. A **45**, 8683 (1992).
[25] N. Boden, J. Clements, K. A. Dawson, K. W. Jolley, and D. Parker, Phys. Rev. Lett. **66**, 2883 (1991).
[26] K. W. Jolley, M. H. Smith, and N. Boden, Chem. Phys. Lett. **162**, 152 (1989).
[27] E. F. Gramsbergen, L. Longa, and W. H. de Jeu, Phys. Rep. **135**, 195 (1986).
[28] S. Kumar, L. J. Yu, and J. D. Litster, Phys. Rev. Lett. **50**, 1672 (1983).
[29] N. Boden, S. A. Corne, P. Halford-Maw, D. Fogarty, and K. W. Jolley, J. Magn. Reson. **98**, 92 (1992).
[30] G. R. Luckhurst, J. Chem. Soc., Faraday Trans. 2 **84**, 961 (1988).
[31] G. S. Attard and G. R. Luckhurst, Liq. Cryst. **2**, 441 (1987).
[32] M. C. Holmes, D. J. Reynolds, and N. Boden, J. Phys. Chem. **91**, 5257 (1987).
[33] H. Iijima, T. Kato, H. Yoshida, and M. Imai, J. Phys. Chem. **102**, 990 (1998).
[34] H. Johannesson, I. Furo, and B. Halle, Phys. Rev. E **53**, 4904 (1996).
[35] Y. M. Shih, H. M. Huang, and C. W. Woo, Mol. Cryst. Liq. Cryst. **34**, 7 (1976).
[36] C.-P. Fan and M. J. Stephen, Phys. Rev. Lett. **25**, 500 (1970).
[37] T. W. Stinson and J. D. Litster, Phys. Rev. Lett. **25**, 503 (1970).
[38] T. W. Stinson and J. D. Litster, J. Appl. Phys. **41**, 996 (1970).
[39] P. G. de Gennes and J. Prost, *The Physics of Liquid Crystals* (Clarendon, Oxford, 1993).
[40] P. K. Mukherjee, J. Phys.: Condens. Matter **10**, 9191 (1998).
[41] W. Guo, T. A. Brown, and B. M. Fung, J. Phys. Chem. **95**, 1829 (1991).
[42] M. A. Bates and D. Frenkel, J. Chem. Phys. **110**, 6553 (1999).
[43] Y. Poggi, J. C. Filippini, and R. Aleonard, Phys. Lett. **57A**, 53 (1976).
[44] Y. Poggi, P. Allen, and J. C. Filippini, Mol. Cryst. Liq. Cryst. **37**, 1 (1976).
[45] Y. Poggi, P. Allen, and R. Aleonarf, Phys. Rev. A **14**, 466 (1976).
[46] J. Thoen and G. Menu, Mol. Cryst. Liq. Cryst. **97**, 163 (1983).
[47] D. Frenkel and R. Eppenga, Phys. Rev. Lett. **49**, 1089 (1982).
[48] R. Eppenga and D. Frenkel, Mol. Phys. **52**, 1303 (1984).
[49] B. Tjipto-Margo and G. T. Evans, J. Chem. Phys. **93**, 4254 (1990).
[50] F. M. van der Kooij and H. N. W. Lekkerkerker, J. Phys. Chem. **102**, 7829 (1998).
[51] D. Parker, Ph.D. thesis, University of Leeds, 1987 (unpublished).